Scaling relations for the length of coaxial oxy-flames with and without swirl

A Degeneve, Ronan Vicquelin, Clément Mirat, B. Labegorre, P. Jourdaine, J. Caudal, Thierry Schuller

37th International Symposium on Combustion

Scaling relations for the length of coaxial oxy-flames with and without swirl

A. Degeneve[a,b,1], R. Vicquelin[a], C. Mirat[a], B. Labegorre[b], P. Jourdaine[b], J. Caudal[b], T. Schuller[a,c]

[a]*Laboratoire EM2C, CNRS, CentraleSupélec, Université Paris-Saclay, 3 rue Joliot Curie 91192 Gif Sur Yvette cedex, France*

[b]*Air Liquide, Centre de recherche Paris Saclay, Chemin de la Porte des Loges, B.P. 126, 78354 Les Loges en Josas, France*

[c]*Institut de Mécanique des Fluides de Toulouse (IMFT), Université de Toulouse, CNRS, INPT, UPS, Toulouse, France*

Colloquium:

Stationnary combustion systems and control of green house gas emissions

Word Count: Method 2, counting from a two-column formatted version of the paper.

Paper length: 8 pages, Equivalent word count: 6200 words

Supplemental material: One page of supplemental material is added.

[1]Corresponding author: Arthur Degeneve, Laboratoire EM2C, CNRS, CentraleSupélec, Université Paris-Saclay, 3 rue Joliot Curie 91192 Gif Sur Yvette cedex, France
Email: arthur.degeneve@centralesupelec.fr

Scaling relations for the length of coaxial oxy-flames with and without swirl

A. Degeneve[a,b,*], R. Vicquelin[a], C. Mirat[a], B. Labegorre[b], P. Jourdaine[b], J. Caudal[b], T. Schuller[a,c]

[a] *Laboratoire EM2C, CNRS, CentraleSupélec, Université Paris-Saclay, 3, rue Joliot Curie, 91192 Gif-sur-Yvette cedex, France*
[b] *Air Liquide, Centre de recherche Paris Saclay, Chemin de la Porte des Loges, B.P. 126, 78354 Les Loges en Josas, France*
[c] *Institut de Mécanique des Fluides de Toulouse (IMFT), Université de Toulouse, CNRS, INPT, UPS, Toulouse, France*

Abstract

An extensive experimental study is carried out to analyze scaling laws for the length of methane oxy-flames stabilized on a coaxial injector. The central methane fuel stream is diluted with N_2, CO_2 and He. The annular air stream is enriched with oxygen and can be impregnated with swirl. Former studies have shown that the stoichiometric mixing length of relatively short flames is controlled by the mixing process taking place in the vicinity of the injector outlet. This property has been used to derive scaling laws at large values of the stoichiometric mixture fraction. It is shown here that the same relation can be extended to methane oxy-flames characterized by small values of the stoichiometric mixture fraction. Flame lengths are determined with OH* chemiluminescence measurements over more than 1000 combinations of momentum ratio, annular swirl level and composition of the inner and outer streams of the coaxial injector. It is found that the lengths of all the flames investigated without swirl collapse on a single line, whose coefficients correspond to within 15% of flame lengths obtained for fuel and oxidizer streams at much larger stoichiometric mixture fractions. This relation is then extended to the case of swirling flames by including the contribution of the tangential velocity in the flow entrainment rate and is found to well reproduce the mixing degree of the two co-axial streams as long as the flow does not exhibit a vortex breakdown bubble. At higher swirl levels, when the flow features a central recirculation region, the flame length is found to also directly depend on the oxygen enrichment in the oxidizer stream.

Keywords:
Coaxial jet, Oxy-combustion, Swirl, Flame length, Turbulence

1. Introduction

Many industrial combustors are powered by co-axial injectors in which the oxidizer and fuel streams are injected separately and expand in a large combustion chamber. It is well known that the mixing degree between the two streams controls the flame length and therefore it has been the topic of numerous investigations [1–10]. The development of technologies such as oxy-combustion needs however to broaden the investigated range of operations and to deepen knowledge of the mixing mechanisms of coaxial jets, in which one of the jets may eventually feature a swirling motion.

It is at this point worth reviewing the current state of knowledge on parameters altering the flame length from co-axial injectors. Regarding diffusion flames, the distance from the injector needed to obtain a stoichiometric fuel and oxidizer mixture well defines the flame length [11]. The pioneering works from Hawthorne *et al.* [12] and Peters and Gottgens [11] have established mixing rules for free single jets exhausting in quiescent atmosphere. For non-buoyant turbulent coaxial jets, mixing is controlled far from the injector by the self-similar behavior of the resulting turbulent jet [3, 13]. This so-called far-field approach allows to well reproduce the topology of methane diffusion flames with high impulsion of the fuel inner jet [4–6]. In this case the stoichiometric mixture fraction z_{st} remains small, leading to long flames far from the inner jet potential core [4, 5].

In many applications, like in H_2-O_2 rocket engines or oxy-combustion, the stoichiometric mixture fraction z_{st} takes relatively large values and the difference between the potential core and stoichiometric lengths reduces. In this regime, another mechanism prevails and mixing is controlled by engulfment of large scale instabilities developing in the shear layer between the central and

*Corresponding author:
Email address: arthur.degeneve@centralesupelec.fr (A. Degeneve)

annular jet streams in the vicinity of the jet potential core [8, 14]. The developments made with this near-field approach has led to the following scaling law for the stoichiometric flame length L_s [8, 9]:

$$\frac{L_S}{d_1} = c_1(J^{1/2}X_{st})^{-1} + c_0 \quad (1)$$

where c_0 and c_1 are positive constants, d_1 is the central injector diameter, X_{st} is the molar stoichiometric mixture fraction and $J = \rho_2 u_2^2/\rho_1 u_1^2$ corresponds to the momentum ratio between the two streams. This relation was found to successfully reproduce the stoichiometric mixing length L_s of co-axial streams with an air jet in the center surrounded by a co-flow of H_2 or CH_4 in non reacting conditions [10].

These results established for cold flows have been extended to consider effects of heat release. The dominant effect of combustion lies in the drop of flow entrainment due to the drop of density in the burnt gases [15]. Tacina and Dahm [15, 16] found that mixing of the inner fuel and the outer oxidizer streams in reacting conditions is equivalent to the non reacting mixing process of the inner fuel with an equivalent outer oxidizer characterized by an effective higher temperature T_2^{eq}. Assuming that the density difference between the two streams due to molar weight is small compared to the effect of temperature, the density of the equivalent jet is defined as $\rho_2^{eq} = (T_2/T_2^{eq})\rho_2$ [15]. This method is used in [9] to collapse data for O_2/H_2 flames with hydrogen in the outer stream ($z_{st} = 0.89$, $X_{st} = 0.33$). Results in non reacting and reacting conditions collapse when the momentum ratio J is replaced by its equivalent J_{eq} defined as:

$$J_{eq} = \frac{\rho_2^{eq}}{\rho_1}\frac{u_2^2}{u_1^2} \quad (2)$$

Scaling laws for the length of methane oxy-flames have been reported so far with contrasted results. Effects of dilution in both the inner and outer streams have not been systematically investigated [17–20]. In many studies, only heuristic corrections are presented when switching from air to oxygen operation [20] and investigations are often limited to regimes with velocities in the inner fuel stream much higher than in the annular stream ($J \ll 1$)[17–20], resulting in long flames where the near-field mechanism does not control mixing. Few studies with higher momentum in the annular stream have been conducted with oxy-flames [19] and N_2-diluted hydrogen flames [13], but no scaling laws are reported. A unified approach consistent with both air- and oxy-condition operations is still missing.

This lack of data has motivated this study conducted for a wide set of operating conditions in which the gas composition in the central and annular streams and the momentum ratio can separately be varied. The first objective of this article is to examine the length of coaxial oxy-flames with a large set of dilution rates in the oxidizer and fuel streams. Attempts are then made to collapse the data with theoretical elements. The second objective is to analyze effects of the swirl level in the annular jet and derive a model which accounts for the resulting turbulence enhancement.

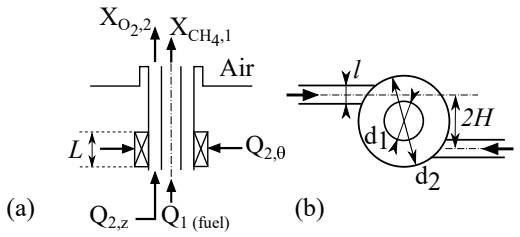

Figure 1: Sketch of the coaxial injector. (a) Axial cut. (b) Transverse cut through the swirler.

2. Experimental setup

The injector sketched in Fig. 1 comprises a central tube of inner diameter $d_1 = 6$ mm and thickness $e = 1$ mm, wherein methane is eventually mixed with a diluent (N_2, CO_2 or He), and an annular injection channel of outer diameter $d_2 = 20$ mm, with an adjustable O_2/N_2 gas composition. A swirl motion can be imposed to the annular stream thanks to tangential slits. The axial and tangential volume flowrates injected in the annular channel are designated respectively by $Q_{2,z}$ and $Q_{2,\theta}$. Assuming a solid-body rotation, the geometrical swirl number S_2 in the annular channel is given by:

$$S_2 = \frac{\pi}{4}\frac{Hd_2}{NlL}\frac{1-(d_2/d_1)^4}{1+Q_{2,z}/Q_{2,\theta}} \quad (3)$$

where H is the distance separating the tangential injection channels from the burner axis, l the width and L the height of the N tangential injection channels. This device was designed to produce geometrical swirl numbers ranging from $S_2 = 0$ to 1.73 with $N = 2$ slits. The central fuel stream is not swirled in this study. The coaxial jet exhausts in quiescent air at ambient pressure, above a back plane at room temperature $T = 300$ K, so as to avoid effects of confinement and heat transfer to the walls. The coaxial injector outlet is elevated 5 mm above the back plane to ease visualization and there is no recess between the central and outer injector outlets. This altitude defines the axial origin $z = 0$.

The flame length is defined as the furthest point on the axis with a combustion reaction [12, 17]. In many cases, the length of diffusion flames is determined by recording its global emission in the visible band [12, 19, 20] or the emission of selected intermediate radicals [9, 17, 18]. In these studies, the flame length is commonly correlated to the stoichiometric mixing length L_S. Given the large range of operating conditions targeted in this work, it is first worth exploring if the OH* emission signal is a good tracer for the length of oxy-flames and if it is well correlated to the stoichiometric mixing length L_S.

Numerical simulations of steady one-dimensional counterflow methane oxy-flames were carried out with the Grimech 3.0 mechanism [21] in [22] and completed with OH* chemistry in [23]. These authors verified that the OH* peak emission from diffusion oxy-flames lies very close to stoichiometry at $z = z_{st}$ for a large range of oxygen enrichments and strain rates. Numerical simulations have also been carried out in this study to verify this property for selected operating points with the same Grimech 3.0 mechanism completed with the chemistry of OH* [23]. They are provided as supplementary material and confirm that both peaks of temperature and OH* lie close to the flame front at $z = z_{st}$, when compared to the flame thickness. Self-similar counterflow equations were solved with an in-house code with identical transport and thermodynamics properties as in the CHEMKIN package and similar numerical algorithms.

The OH* images are recorded with a 16 bit intensified CCD camera (ICCD, Princeton, PI-MAX4, 1024 × 1024 pixels) equipped with an UV objective (Nikkor 105 mm) and a 10 nm bandpass filter centered at 310 nm (Asahi XBPA310-Bandpass). Line of sight integrated averaged fields of OH* emission are determined from 30 snapshots each with an exposure time of 200 ms. Statistical convergence of the mean OH* intensity is systematically verified.

The Otsu thresholding method [24] is chosen here to infer the flame front location from the OH* images as in [25, 26]. Examples without swirl are shown in Fig. 2 and effects of swirl are illustrated in Fig. 3. The stoichiometric mixing length L_S is determined as the highest point of the Otsu contour, which is found to lie along the burner centerline, except for the highly swirled flames featuring a central recirculation zone. A sensitivity analysis has been carried out to examine changes of L_S when varying the image brightness and contrast. Different exposure times and camera apertures were tested. It appears that the largest variations of L_S are limited to within 5%. The method is also validated in section 4 by comparing the results with the stoichiometric mixing length determined from measurements made with acetone laser induced fluorescence [9, 10].

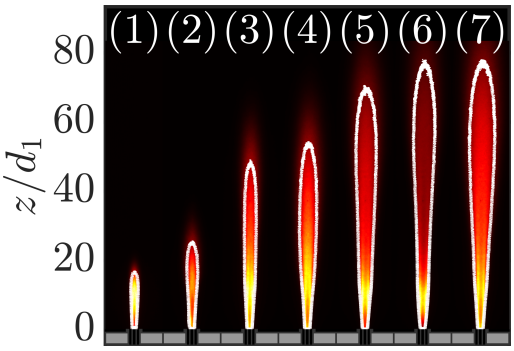

Figure 2: OH* intensity distribution of selected flames from dataset D2 in Tab. 1 and increasing Φ_m values. Numbers refer to Fig. 4b. White contours indicate the Otsu threshold used to determine L_S.

3. Operating conditions

Changes of the flame length are investigated by modifying the momentum ratio J between the two streams and the stoichiometric (molar) mixture fraction X_{st}. This is made by varying the bulk flow velocity u_1 from the central stream and the gas composition of the central and annular streams (see Tab. 1). All the following experiments are conducted at high Reynolds numbers Re_2 to get a fully developed turbulent flow in the annular channel. In this case, the flame length L_S does not depend on Re_2 [9]. The fuel in the central jet is also always the deficient reactant to avoid combustion between the excess of fuel in the burnt gases with ambient air. Therefore, only flames at globally lean conditions are considered here.

Table 1: Ranges of operations explored grouped by dataset. N_f is the number of investigated flames in each group. The central CH_4 stream and the annular O_2 stream are diluted with N_2 except for dataset D4 where fuel dilution is also made with He or CO_2.

Dataset	J	$X_{CH_4,1}$	$X_{O_2,2}$	X_{st}	Z_{st}	$T_s[K]$	S_2	Re_2	N_f
D1	0.2-16	0.40-0.93	0.47	0.20-0.37	0.12 -0.31	2630-2780	0	12000	61
D2	0.2-16	0.34-1	0.37-0.67	0.16-0.50	0.09-0.43	2570-2930	0	12000	174
D3	0.2-16	0.33-1	0.37	0.16-0.36	0.09-0.31	2450-2660	0.4	12000	138
D4	0.2-16	0.33-1	0.37	0.16-0.36	0.09-0.31	2450-2670	0-1	15000	294
D5	0.5-12	0.62-1	0.37	0.16-0.23	0.09-0.17	2600-2660	0-1.5	15000	83
D6	0.4-16	0.30-0.90	0.33 -0.57	0.12-0.37	0.09-0.31	2260-2864	0.8	15000	231

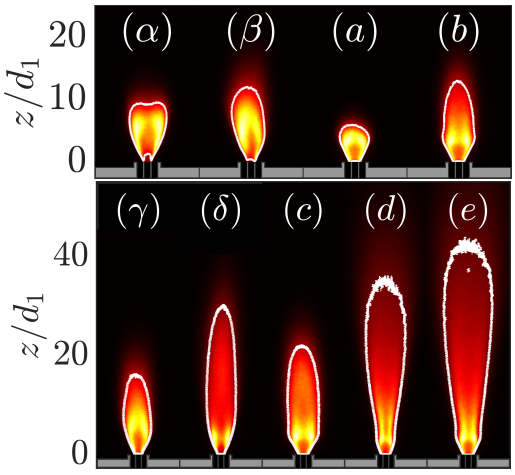

Figure 3: OH* intensity distribution of selected flames from datasets D5 and D6 in Tab. 1 with high annular swirl levels S_2. Latin letters refer to data shown in Fig. 7. Greek letters make references to data shown in Fig. 8. White contours indicate the Otsu threshold used to determine L_S.

Aside from their effect on the flame length, O_2 enrichment and fuel dilution are known to greatly affect flame stabilization. For instance, Wanatabe *et al.* [27] showed that replacing N_2 by CO_2 in twin premixed oxy-flames can increase or decrease the extinction strain rate depending on the equivalence ratio. Chen and Axelbaum [28] showed that increasing the stoichiometric mixture fraction z_{st} drastically increases the extinction limits of counterflow diffusion flames. For these reasons, only flames well attached to the nozzle are considered in this work. This has been achieved with a high degree of O_2 enrichment in the outer stream: $X_{O_2,2} \geq 0.37$ (except for D6 dataset), and without using any bluff-body, confinement or pilot flame, as in [19, 20]. Two decades of the momentum ratio J are covered in the following experiments. High levels of fuel dilution in the inner stream and various levels of O_2 enrichment in the outer injection channel are examined.

Typical results for non-swirling flames are presented in Fig. 2. They all feature a diffusion flame structure attached to the edge of the central injector and their length changes by a factor four. Swirled flames are shorter in Fig. 3 and their opening angle widens as the swirl number S_2 increases.

The dimensionless streamwise coordinate ξ_F from [1] based on the mixing length is of the order of 0.5 indicating that buoyancy effects can be neglected for all configurations explored in this work.

4. Oxy-flames without annular swirl

In the following experiments the swirl level is set to zero $S_2 = 0$. The momentum ratio J and the methane molar fraction $X_{CH_4,1}$ in the central stream are varied. The flame length L_s deduced from the images is made dimensionless with the central injector diameter d_1 and its evolution is examined as a function of the near-field parameter $\Phi_m = (J_{eq}{}^{1/2} X_{st})^{-1}$, where J_{eq} denotes the equivalent momentum ratio from Eq. (2).

Figure 4a shows results from dataset D1 in Tab. 1 in which the oxygen enrichment is set to $X_{O_2,2} = 0.47$ in the annular stream. Data are plotted for fixed methane molar fractions $X_{CH_4,1}$ varying from 0.40 to 0.93 in the inner jet, the fuel being diluted with nitrogen. Effects of the oxygen enrichment in the annular stream with respect to air are examined in Fig. 4b for $X_{O_2,2}$ =0.37 to 0.67. The spread of the color legends emphasizes the broad ranges covered by $X_{CH4,1}$ and $X_{O_2,2}$ in Fig. 4.

Flame lengths L_S from datasets D1 and D2 all collapse on the same curve in Fig. 4 when results are plotted as a function of Φ_m. Modifying the composition X_{st} or the momentum ratio J has a distinct influence on L_S. Increasing the fraction of nitrogen N_2 in the inner stream or of oxygen O_2 in the annular jet increases the stoichiometric mixture fraction X_{st}, which moves the stoichiometric mixing length L_S closer to the potential core of the central jet. Secondly, increasing the annular momentum ratio J increases the level of turbulent diffusion, which reduces the length of the potential core of the central jet and enhances mixing of both streams. These figures confirm that the two mechanisms successfully account for the measured flame lengths through the use of Φ_m. The range of stoichiometric mixture fractions $0.09 \leq z_{st} \leq 0.43$ covered in this study is wider than previous studies [9, 10] conducted with H_2/O_2 and $0.80 \leq z_{st} \leq 0.95$. The linear relationship of the flame length with Φ_m is still valid for the lowest z_{st} value corresponding to $X_{CH_4,1} = 1$ and $X_{O_2,2} = 0.37$. Equation (1) derived with arguments regarding the development of shear layer instabilities near the inner jet potential core, a situation where z_{st} is large [8], appears to remain valid for a large range of z_{st} values. This observation deserves further investigations to understand its roots.

Figures 4a and 4b also indicate that the slope of L_S/d_1 deviates from the linear behavior when $\Phi_m \geq 20$. The saturation observed at high Φ_m values does not appear to be a bias of diagnostic. The OH* emission is not deteriorated for flames 6 and 7 in Fig. 2 and the Otsu contour still well delineates the flame reaction front. In the asymptotical regime reached for vanishingly small impulsion ratios $J \to 0$, turbulent mixing is solely con-

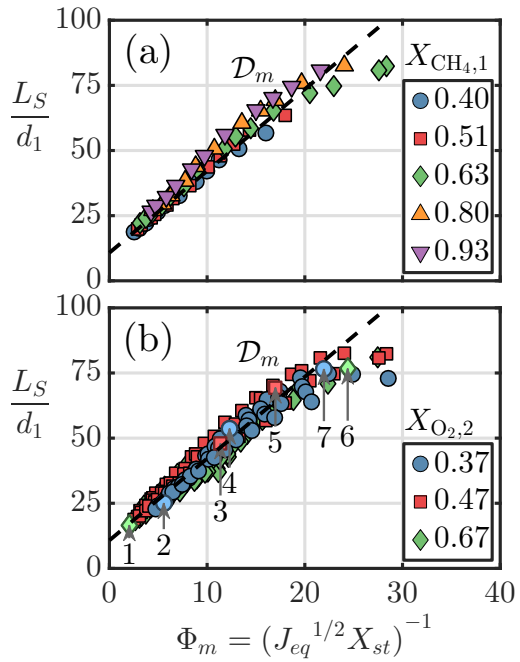

Figure 4: Flame lengths from datasets D1 (top graph) and D2 (bottom graph) in Tab. 1 obtained without swirl $S_2 = 0$. $\mathcal{D}_m$: Eq. (4).

trolled by the inner jet velocity u_1 and the flame length does not depend anymore on the velocity ratio u_2/u_1. In this limit case, one recovers the scaling law from a free single jet exhausting in quiescent air [11, 12]. The transition for the relevant shear velocity from u_2 to u_1 was already mentioned in [8], but could not be observed in [9, 10], where flames smaller than $L_S/d_1 = 55$ are investigated. The deviation from the linear behavior for $L_S/d_1 \geq 75$ in Fig. 4 is attributed to the transition in a regime where mixing is controlled by the inner jet turbulence.

In the linear regime observed for $\Phi_m < 20$, a regression of the data $\mathcal{D}_m$ in Figs. 4a-b yields :

$$\mathcal{D}_m : \frac{L_S}{d_1} = b_1 (J_{eq}{}^{1/2} X_{st})^{-1} + b_0 \qquad (4)$$

where $b_1 = 3.1$ and $b_0 = 10.7$. These results obtained for N_2-diluted CH_4/O_2-enriched flames are found to be in good agreement with measurements from Schumaker and Driscoll [9] who report $b_1 = 2.7$ in their H_2/O_2 configuration, in which the fuel is the annular jet. Besides, they also found that the constant b_0 used to improve the linear fit mainly depends on the injector geometry and therefore cannot be compared. The line $\mathcal{D}_m$ from Eq. (4) serves as a reference in the remaining part of this article.

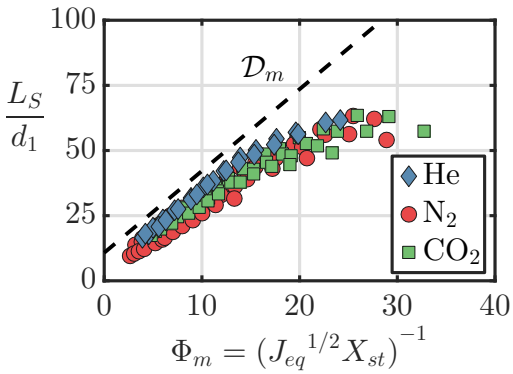

Figure 5: Flame lengths from dataset D3 in Tab. 1 obtained for $X_{O_2,2} = 0.37$ and $S_2 = 0.4$. $\mathcal{D}_m$: Eq. (4).

5. Oxy-flames with annular swirl

Effects of the swirl level in the annular stream are now examined. Results are first presented for the dataset D3 in Tab. 1 obtained for a moderate swirl level $S_2 = 0.4$ and a slight oxygen enrichment $X_{O_2,2} = 0.37$ of the oxidizer stream. They are grouped in Fig. 5. Nitrogen N_2 used to dilute the central jet is here alternatively replaced by CO_2 and He exhibiting large differences in molar weights. The measured flame lengths L_s collapse in these cases again on a single curve in Fig. 5 when data are plotted as a function of Φ_m, which therefore remains the proper parameter to switch from one fuel stream diluent to another. The stoichiometric mixing lengths lie however below the line $\mathcal{D}_m$ found for the non-swirling flames ($S_2 = 0$). This means that addition of the swirl $S_2 = 0.4$ has uniformly reduced the stoichiometric lengths L_s of all flames of dataset D3. Swirling the annular stream is indeed known to enhance the mixing rate and reduce the stoichiometric mixing length [2, 29].

Changes of the annular swirl level S_2 are studied in Fig. 6 for the dataset D4 in Tab. 1 obtained for a fixed O_2 enrichment $X_{O_2,2} = 0.37$ in the outer stream. Each dataset color corresponds to a different swirl number S_2. For a fixed swirl level S_2, the flame lengths L_S collapse again on a single curve as J and X_{st} vary, even at high swirl numbers $S_2 > 0.6$. For a fixed value of the mixing parameter Φ_m, the flame length reduces monotonically as the swirl number S_2 increases.

This behavior may be accounted for by considering the azimuthal velocity $u_{2,\theta}$ to estimate the turbulent velocity scale within the annular jet:

$$u' \sim |\mathbf{u_2}| \simeq u_2 \left(1 + (kS_2)^2\right)^{1/2} \qquad (5)$$

where k is defined as $u_{\theta,2}/u_2 = kS_2$. The definition of

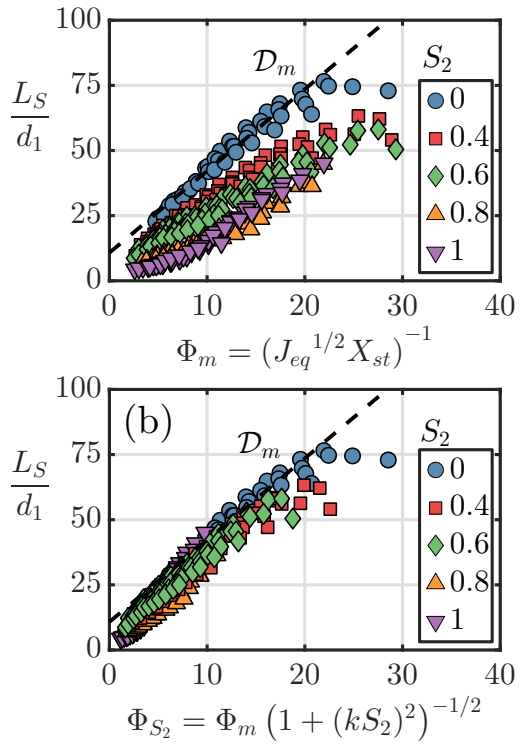

Figure 6: Flame lengths from dataset D4 in Tab. 1. Top : Original scaling Φ_m from [8, 14]. Bottom : New model Φ_{S_2} accounting for the swirl level S_2 in the outer stream. $\mathcal{D}_m$: Eq. (4).

the geometrical swirl number in Eq. (3) with a solid-body rotation yields $k = 2/\left(1 + (d_1/d_2)^2\right)$. This theoretical value is retained in Eq. (5) to account for turbulence enhancement due to swirl in the outer jet. This allows to define a new mixing variable Φ_{S_2}:

$$\Phi_{S_2} = \Phi_m \left(1 + (kS_2)^2\right)^{-1/2} \tag{6}$$

The data in Fig. 6b again roughly collapse on $\mathcal{D}_m$ established for non-swirling flames provided that Φ_m is replaced by Φ_{S_2} in Eq. (4) :

$$\frac{L_S}{d_1} = b_1 \Phi_{S_2} + b_0 \tag{7}$$

where the values for b_0 and b_1 are left unchanged. These results indicate that the near-field approach [8, 14] can be extended to the case of swirling flames, in which the main effect of swirl is the enhancement of turbulent mixing between the central and annular jets. A closer look at the data shows that the scaling law worsen for high swirl levels. Increasing the outer stream swirl number S_2 from small to moderate values leads to an increase of turbulent diffusion between the two jets, but a sudden change of the flow topology appears at higher values due to vortex breakdown with the formation of a central recirculation zone (CRZ). As reported in [2], the flame length drastically drops down to $L_S/d_1 = 5$ at high swirl levels.

This flow transition is examined by considering experiments made for the dataset D5 in Tab. 1. In these experiments the mixing parameter Φ_m (corresponding to $\Phi_{S_2=0}$) remains constant and only the annular swirl level S_2 is varied. The flame lengths are reported as a function of S_2 in Fig. 7 at different fixed values for Φ_m. Predictions from Eq. (7) are superimposed to the experimental data. Increasing the annular swirl S_2 leads to a decrease of the flame length L_S in a nonlinear fashion, which is well reproduced by Eq. (7) for swirl numbers lower than $S_2 \leq 0.5$.

The extended model Eq. (7) also well reproduces the stoichiometric mixing length of the highly swirled flames, but only at high Φ_m values. When both the annular impulsion ratio J and the swirl number S_2 are high enough, vortex breakdown drastically alters the flame topology with the formation of a CRZ leading to a much shorter flame length. This is exemplified by flame a featuring a CRZ compared to flames d and e remaining in the jet-like regime in Fig. (3). This regime transition is in agreement with results from Chen and Driscoll [30], who mapped the apparition of the CRZ in a $(1/J, S_2)$ diagram. They found that for $S_2 > 0.7$, the transition from a jet-like to a strongly recirculating regime occurs for $J > J_c \simeq 1$, and the critical threshold J_c depends on S_2 for $S_2 < 0.7$. This condition is reproduced in Fig. (7), where data for flames expected in a jet-like regime are represented by symbols with a thickened black contour. Flames in a regime with a CRZ according to [30] are drawn with a thin contour. Equation (7) reproduces the measured flame lengths only in the jet-like regime. This corroborates that Eq. (7) well models mixing enhancement in the jet-like regime due to the additional turbulence generated by the rotation of the outer swirling jet, but does not hold in the CRZ regime, in which mixing is mainly controlled by recirculation of the gases in the central region of the flow.

Physics based scaling relations for the flame length in highly recirculating flows have been proposed for methane/air flames by means of velocity measurements in the recirculating vortex [2, 30]. It is found here that fuel dilution and oxygen enrichment further increase the complexity of the mixing dynamics for these flames featuring a central vortex bubble, for which Eq. (7) fails to reproduce the stoichiometric mixing length.

Complementary measurements corresponding to the dataset D6 in Tab. 1 are analyzed for a swirl number $S_2 = 0.8$. The O_2 enrichment in the annular stream

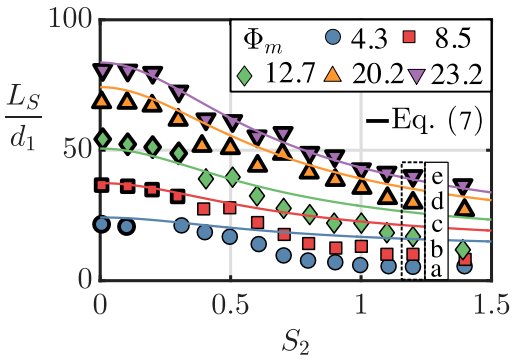

Figure 7: Flame lengths from the dataset D5 in Tab. 1 as a function of the swirl number S_2 for different values of mixing parameter Φ_m. Solid lines correspond to predictions from Eq. (7). Symbols with thickened contour designate flames in jet-like regime according to [30].

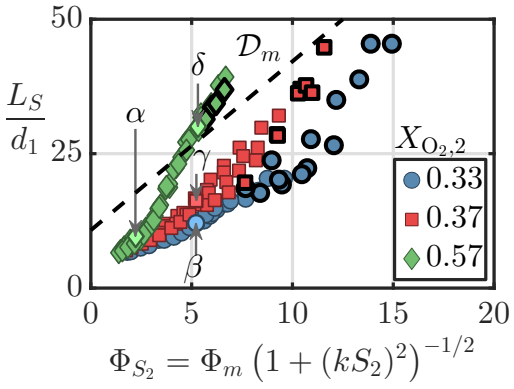

Figure 8: Flame lengths from the dataset D6 in Tab. 1 obtained for $S_2 = 0.8$ and different oxygen molar fractions $X_{O_2,2}$ in the annular stream. $\mathcal{D}_m$: Eq. (4).

is varied from $X_{O_2,2} = 0.33$ to 0.57. The central fuel stream is diluted with N_2 with $X_{CH_4,1} = 0.30$ to 0.90. Flame lengths are plotted in Fig. 8 with respect to Φ_{S_2}, which again appears as a suitable parameter associated to changes of the central fuel jet composition $X_{CH_4,1}$ and momentum ratio J, but the results are found to also depend on the oxygen enrichment $X_{O_2,2}$ in the annular stream. Flames corresponding to β, γ and δ in Fig. 8 are displayed in Fig. 3. They share the same value Φ_{S_2} but feature different stoichiometric mixing lengths. Flame β is small and compact in Fig. 3, whereas flame δ is much longer. As this feature is left unexplained by the Eq. (7) developed in this work, modifications of the mixing degree are attributed to the presence of the central recirculating bubble, as mentioned in [2, 30]. Besides, the diagram established for the CRZ of methane-air flames in [30] does not account for the following observation with oxy-flames: flame γ has a higher momentum ratio J than flame β, but flame β is smaller than flame γ in Fig. 3.

A more detailed description of the interaction between the flow in the CRZ and the oxidizer annular stream is needed to explain the topology of these flames, but the O_2 concentration in the annular stream seems to be an independent parameter that needs to be considered for highly-recirculating flames.

Conclusion

Modifications of the flame length L_s of methane oxygen enriched flames stabilized on coaxial injectors have been investigated over a large set of parameters using OH* chemiluminescence measurements. Effects of dilution of the central fuel stream have first been investigated by varying the fuel molar fraction $0.33 \leq X_{CH_4,1} \leq 1$ and the diluent nature N_2, CO_2 and He. Secondly, experiments have been reported for momentum ratio $J = \rho_2 u_2^2/\rho_1 u_1^2$ covering a broad range $0.2 \leq J \leq 16$. Third, effects of oxygen enrichment in the annular oxidizer stream have been investigated from $0.37 \leq X_{O_2,2} \leq 0.67$. Finally, the swirl number of the annular stream has also been varied up to $S_2 \leq 1.5$. This parametric analysis enabled to explore the lengths of oxy-flames through more than 1000 combinations.

In the absence of swirl, the relation proposed in [9] has been used to successfully reduce the data for the flame lengths L_S on a single line as a function of a single dimensionless mixing parameter corresponding to the inverse of the product of the stoichiometric mixture fraction X_{st} and the square root of the equivalent momentum ratio J_{eq}. The slope of this line has been found to match the one reported for O_2/H_2 flames with $0.80 \leq z_{st} \leq 0.95$ in [9, 10] within 15%. The current experiments validate this relation for oxy-methane flames featuring a smaller stoichiometric mixture fraction $0.09 \leq z_{st} \leq 0.43$.

With swirl, the same type of relation with a correction taking into account enhancement of turbulent diffusion due to the azimuthal flow component has been found to well reproduce the length of swirling flames before the apparition of a central vortex bubble. At high swirl levels characterized by a central recirculating flow, it has been found that the flame length also separately depends on the oxygen enrichment in the oxidizer stream.

The current work provides a large database for the lengths of coaxial oxy-flames. Given the broad range of operating conditions, the extended scaling law Eq. (7) may be used to ease the design of co-axial injectors from oxy-burners, with eventually a slight swirl in outer stream. Furthermore, the data gathered in this work also

yields a large validation database for simulation of stoichiometric mixing lengths in oxy-flames.

Acknowledgments

This work is supported by the Air Liquide, CentraleSupélec and CNRS Chair on oxy-combustion and heat transfer for energy and environment and by the OXYTEC project (ANR-12-CHIN- 0001) from l'Agence Nationale de la Recherche.

References

[1] H. Becker, S. Yamazaki, Combust. Flame 33 (1978) 123–149.
[2] R.-H. Chen, J. F. Driscoll, Proc. Comb. Inst. 22 (1989) 531–540.
[3] W. Dahm, A. Mayman, AIAA J. 28 (1990) 1157–1162.
[4] R.-H. Chen, J. F. Driscoll, Proc. Comb. Inst. 23 (1991) 281–288.
[5] J. F. Driscoll, R.-H. Chen, Y. Yoon, Combust. Flame 88 (1992) 37–49.
[6] T. Cheng, Y.-C. Chao, D.-C. Wu, T. Yuan, C.-C. Lu, C.-K. Cheng, J.-M. Chang, Proc. Comb. Inst. 27 (1998) 1229–1237.
[7] M. Favre-Marinet, E. Camano, J. Sarboch, Exp. Fluids 26 (1999) 97–106.
[8] E. Villermaux, H. Rehab, J. Fluid. Mech. 425 (2000) 161–185.
[9] S. A. Schumaker, J. F. Driscoll, Proc. Comb. Inst. 32 (2009) 1655–1662.
[10] S. Alexander Schumaker, J. F. Driscoll, Phys. Fluids 24 (2012) 055101.
[11] N. Peters, J. Göttgens, Combust. Flame 85 (1991) 206–214.
[12] W. Hawthorne, D. Weddell, H. Hottel, Proc. Comb. Inst. 3 (1948) 266–288.
[13] N. Weiland, R.-H. Chen, P. Strakey, Proc. Comb. Inst. 33 (2011) 2983–2989.
[14] H. Rehab, E. Villermaux, E. Hopfinger, J. Fluid. Mech. 345 (1997) 357–381.
[15] K. M. Tacina, W. J. Dahm, J. Fluid. Mech. 415 (2000) 23–44.
[16] W. J. Dahm, J. Fluid. Mech. 540 (2005) 1–19.
[17] J. Sautet, L. Salentey, M. Ditaranto, J. Samaniego, Combust. Sci. Technol. 166 (2001) 131–150.
[18] M. Ditaranto, J. Sautet, J. Samaniego, Exp. Fluids 30 (2001) 253–261.
[19] H. K. Kim, Y. Kim, S. M. Lee, K. Y. Ahn, Energy Fuels 20 (2006) 2125–2130.
[20] H. K. Kim, Y. Kim, S. M. Lee, K. Y. Ahn, Energy Fuels 21 (2007) 1459–1467.
[21] G. P. Smith, D. M. Golden, M. Frenklach, N. W. Moriarty, B. Eiteneer, M. Goldenberg, C. T. Bowman, R. K. Hanson, S. Song, W. Gardiner Jr, et al., URL http://www. me. berkeley. edu/gri_mech (2011).
[22] K. Maruta, K. Abe, S. Hasegawa, S. Maruyama, J. Sato, Proc. of the Comb. Inst. 31 (2007) 1223–1230.
[23] M. De Leo, A. Saveliev, L. A. Kennedy, S. A. Zelepouga, Combust. and Flame 149 (2007) 435–447.
[24] N. Otsu, IEEE Trans. Syst. Man Cybern 9 (1979) 62–66.
[25] X. Zhang, L. Hu, W. Zhu, X. Zhang, L. Yang, Appl. Therm. Eng. 73 (2014) 15–22.
[26] Q. Wang, L. Hu, X. Zhang, X. Zhang, S. Lu, H. Ding, Energy Convers. Manag. 106 (2015) 703–708.
[27] H. Watanabe, S. J. Shanbhogue, A. F. Ghoniem, ASME Turbo Expo (2015) V04BT04A014.
[28] R. Chen, R. Axelbaum, Combust. and Flame 142 (2005) 62–71.
[29] M. Ribeiro, J. Whitelaw, J. Fluid. Mech. 96 (1980) 769–795.
[30] R.-H. Chen, J. F. Driscoll, J. Kelly, M. Namazian, R. Schefer, Combust. Sci. Technol. 71 (1990) 197–217.